frontiers | Frontiers in Marine Science

TYPE Original Research
PUBLISHED 21 July 2023
DOI 10.3389/fmars.2023.1228933

OPEN ACCESS

EDITED BY
Yi-Feng Li,
Shanghai Ocean University, China

REVIEWED BY
Sang Yoon Lee,
Cellqua., Inc, Republic of Korea
Chunyan Zhao,
Qingdao Agricultural University, China

*CORRESPONDENCE
Zhongliang Wang
zhongliangwang@vip.163.com

RECEIVED 25 May 2023
ACCEPTED 05 July 2023
PUBLISHED 21 July 2023

CITATION
Chen Z, Huang B, Yan Z, Hong Y, Zhao M, Jin M, Zheng A and Wang Z (2023) Genome–wide expression profile analysis of the NHE and NKA gene family in *Rachycentron canadum* (Linnaeus, 1766) and its response to salinity adaptation. *Front. Mar. Sci.* 10:1228933. doi: 10.3389/fmars.2023.1228933

Genome–wide expression profile analysis of the NHE and NKA gene family in *Rachycentron canadum* (Linnaeus, 1766) and its response to salinity adaptation

Zongfa Chen[1], Baosong Huang[2], Ziqi Yan[1], Yujie Hong[1], Mingming Zhao[1], Minxuan Jin[1], Anna Zheng[1] and Zhongliang Wang[1]*

[1]College of Fisheies, Guangdong Qcean University, Zhanjiang, China, [2]Agricultural Service Center, Agricultural and Rural Bureau of Sanjiao Town, Zhongshan, China

NHE and NKA are important regulators of ion transport in fish and play a pivotal role in maintaining osmotic balance and adapting to salinity changes. However, no systematic identification and functional analysis has been conducted for NHEs and NKAs in the cobia (*Rachycentron canadum*), a commercially important worldwide flatfish. Herein,12 NHE genes were found to be distributed on 10 chromosomes and 12 NKA genes were found to be distributed on 9 chromosomes were identified in the *R. canadum* at the genome-wide level. Histopathological examination of the gills demonstrated the response of gill lamellae and chloride cells to salinity, while the microstructure of the intestine and kidney exhibited changes associated with salinity. The findings show that members of the NHE and NKA gene families are widely distributed in gill, brain, and heart tissues. Specifically, NHE genes exhibited high expression levels in the gill, somatic kidney, and brain, whereas NKA genes displayed prominent expression in the gill, brain, and heart. Moreover, salinity adaptation experiments were conducted to examine the response of NHE and NKA genes. In the intestine, *NHE1* expression was significantly upregulated following both high and low salt stimulation, while the somatic kidney exhibited a proportional response to changes in salinity. Notably, a significant downward trend in *NHE2c* expression was observed in the gill, intestine, and somatic kidney with increasing salinity. Following low-salt acclimation, *NKAα1b* and *NKAβ3a* were significantly down-regulated in the gill, whereas *NKAα3a* and *NKAβ3a* displayed significant up-regulation and down-regulation in the intestine, respectively. In the somatic kidney, *NKAα1b*, *NKAα3a*, and *NKAβ3a* were significantly up-regulated. During high-salt acclimation, the expression patterns of *NKAα1b* and *NKAβ3a* in the gill were consistent with those observed during low-salt acclimation, while *NKAα3a* and *NKAβ1b* exhibited significant upregulation. Our findings underscore the high conservation of NHE and NKA gene family members in *R. canadum* and highlight tissue-

specific expression patterns and their responses to salinity changes. These results provide valuable insights into the molecular mechanisms governing ion transport and osmoregulation in *R. canadum*, contributing to the development of novel strategies for enhancing aquaculture practices of this species.

KEYWORDS

***Rachycentron canadum*, salinity adaptation, NHE, NKA, histopathology, RNA-seq, qRT-PCR**

1 Introduction

The cobia, *Rachycentron canadum*, is a euryhaline teleost known for its ability to tolerate a wide range of salinity levels, ranging from 22.5 to 44.5 ‰, and it exhibits excellent growth performance (Shaffer and Nakamura, 1989; Smith, 1995). In addition to its fast growth rate, *R. canadum* is a carnivorous fish species highly valued for its delicious meat, nutritional content, and robust resistance. As a result, *R. canadum* has become an important mariculture species in the southeast coast of China (Zhou et al., 2006; Chen et al., 2009). However, the culture of *R. canadum* in seawater nets is vulnerable to extreme weather conditions such as typhoons, heavy rains, and cold fronts. The churning of upwelling and surface seawater can lead to significant fluctuations in seawater salinity and temperature, which have a significant impact on the growth and survival of teleost (Benetti et al., 2021). Salinity is one of the key environmental factors that affect the growth and reproduction of fish (Zhang et al., 2017). Teleost can be classified into euryhaline and non-euryhaline species based on their salinity tolerance. Euryhaline teleost often have well-developed mechanisms of osmoregulation that activate osmoregulatory cells, ion channels, enzymes, and hormones in response to salinity stress, allowing them to survive and thrive in a wide range of salinity levels (Fiol and Kültz, 2007; Holmes et al., 2022). Therefore, studying the salinity adaptation mechanisms of euryhaline teleost can provide a theoretical basis for understanding how they maintain organismal homeostasis in different salinity environments.

Euryhaline teleosts are able to adapt to various salinity levels by regulating ion transport, neuroendocrine function, and energy metabolism through osmoregulatory organs such as the gills, intestines, and kidneys (Yamaguchi et al., 2018). At the molecular level, specific genes have been identified as playing a role in regulating salinity adaptation. These genes include ion transporters such as the sodium potassium pump (NKA), Na^+/K^+/$2Cl^-$ cotransporter 1 (*NKCC1*), Na^+/H^+ exchanger 3 (*NHE3*), Na^+/Cl^- cotransporters (NCC), and cystic fibrosis transmembrane conductance regulator (CFTR) (Marshall, 2011; Hwang et al., 2018). In addition, endocrine hormone genes such as growth hormone (GH), hydrocortisone (COR), prolactin (PRL), and insulin-like growth factor-1 (IGF-1) have also been implicated in the regulation of osmolarity (Jia and Lu, 2016).

NHE proteins are widely distributed ion transporter protein, that play a crucial role in regulating Na^+ and H^+ concentration gradients, which is important for physiological processes (Orlowski and Grinstein, 2004). Members of the *NHE* gene family are involved in a range of cellular processes, including intracellular acid-base homeostasis, cell volume regulation, and Na^+ reabsorption in the kidney and gastrointestine (Counillon and Pouysségur, 2000). In studies on osmolarity in fish, *NHE1*, *NHE2*, and *NHE3* are commonly considered as main candidate genes of the NHE family, with research primarily focused on exploring their relationship with dynamic pH balance, osmolarity homeostasis, and ammonia excretion activity (Edwards et al., 2005).

During salinity acclimation, euryhaline teleosts maintain intracellular homeostasis through the action of ion transport proteins and channels mediated by Na^+/K^+-ATPase (NKA) in the gills (Upling, 2020). NKA is a transmembrane protein composed of α and β subunits that are widely distributed in the gill filaments and body kidneys of fish (Han et al., 2022). It mainly relies on the energy generated by ATP hydrolysis to regulate ion concentration homeostasis in the body, achieve active transmembrane transport of Na^+ and K^+, maintain cellular ion homeostasis, and can be used as an important indicator of osmotic pressure regulation in fish (Jiang et al., 2022). In addition, a study on the salinity experiments of migratory Arctic charr(*Salvelinus alpinus*) suggested that inefficient regulation of osmolality may be due to the failure of *NKAα1b* expression (Bystriansky et al., 2007). NKA activity is closely related to environmental salinity (Yang et al., 2022). Generally, in teleost, NKA activity is positively correlated with increasing salinity. For instance, juvenile Turbot(*Scophthalmus maximus*) showed that gill filament NKA activity and plasma osmolality were highest at a salinity of 33.5 ‰ and lowest at 15 ‰ (Imsland et al., 2003). In *Gadus morhua*, *NKAα* expression in gill filaments and body kidneys significantly decreased in hypoosmotic acclimation experiments, while showing an increasing trend in hypertonic water bodies (Larsen et al., 2012). Furthermore, (Shi et al., 2017) investigated the effect of salinity gradient on *Epinephelus moara* and found that NKA activity initially increased and then decreased in all treatment groups (except the 9‰ group) with a sudden decrease in salinity, while the 9‰ group always showed a decrease in NKA enzyme activity, suggesting that very low salinity leads to a decrease in NKA activity, impaired ion transport efficiency in the gills, and prevents excessive ion loss. The pattern of changes in NKA enzyme activity in the gill filaments and liver of juvenile *Amphiprion clarkii* was consistent, with a constant increase within 24 h of low salt stress and a return to

normal or slightly below normal enzyme activity at 48 h and 96 h (Hu et al., 2016). In a seawater desalination experiment with *Lateolabrax japonicus*, gill tissue NKA enzyme activity initially decreased and then increased, following a "U" shape. During the desalination adaptation phase, the activity gradually recovered and stabilized but remained lower than the control group (salinity 30), with a significant difference between the two groups (Zhang et al., 2018). However, the change pattern of NKA activity in teleost was inconsistent, affected by the intensity of salinity adaptation and could be divided into two contradictory types: positive and negative correlation of salinity change. The former, such as *A. clarkii*, *Oreochromis mossambicus*, and *E. moara*, and the latter, such as *Cleisthenes herzensteini* and *Sparus macrocephlus*, may be related to the strength of osmotic stress tolerance of the species (Lin et al., 2006). Additionally, it has been suggested that NKA activity reaches a minimum when the salinity of the water column reaches the isotonic point in fish (Wang et al., 2011). Differences in osmoregulatory capacity and regulation in different fish species, changes in NKA activity involving individual development (adults vs. juveniles) and salinity adaptation patterns (acute vs. chronic, long-term vs. short-term), are closely related to species evolution.

In this study, we conducted a comprehensive analysis of the NHE and NKA gene families in *R. canadum* to investigate their roles in osmoregulation. Our objectives included identifying and characterizing the members of these gene families using genomic data. We examined the conserved structures of the genes, established an evolutionary tree for the species, and performed transcriptome sequencing to explore the expression patterns of the NHE and NKA gene families in *R. canadum* under various salinity conditions. This research provides valuable insights into the involvement of these gene families in osmoregulation and contributes to our understanding of how *R. canadum* adapts to different salinity environments.

2 Materials and methods

2.1 Experimental fish and sampling

The fish used for the experiment were the juvenile fish artificially hatched and cultured by our group. The fish were temporarily kept in a bucket of 1.5 cubic meters of water in a salinity of 28-30‰, a water temperature of 26-28 °C, and a DO of not less than 6 mg·L^{-1}. 180 fish of uniform size, healthy and vigorous with no damage on the body surface were selected for the salinity adaptation experiment after one week of temporary rearing, and the initial weight of the fish was 9.74 ± 0.85 g. The fish were divided into 10‰ salinity group, 30‰ salinity group and 35‰ salinity group with three biological replicates in each group. The fish were cultured in 9 buckets of 500 L size for 4 weeks, with 20 fish randomly placed in each bucket. The culture water salinity was adjusted downward by 4‰/d using fully aerated dechlorinated fresh water or upward by 4‰/d using sea crystals until the salinity of the experimental group reached the preset salinity and then the experiment was officially started. During the culture period, the water was fed twice daily with 6% body weight of commercial compound feed (46% crude protein and 8% crude lipid) without interruption of aeration and the water exchange rate was 30%.

Two sampling were conducted. In the first sampling, five *R. canadum* were randomly selected after seven days of culture, and eight tissues, including gill, intestine, body kidney, brain, stomach, muscle, spleen, and heart, were collected after anesthesia with eugenol (200 mg/L) for tissue distribution assay. In the second sampling, after four weeks of culture, five fish were randomly selected from each barrel, with a total of 15 fish. Among them,6 fish were anesthetized and three tissues of gill, intestine, and body kidney were taken for phenotypic analysis and qPCR detection, and 9 fish were mixed for transcriptome sequencing. All molecular samples were snap frozen in liquid nitrogen and stored at -80 °C after collection.

2.2 HE staining

The fresh tissue was fixed using paraformaldehyde (4%) for 24 h. Afterwards, the tissue was orderly dehydrated using gradient alcohol, and the wax-soaked tissue was embedded in the embedding machine. And further the tissue was cut into slices with its thickness 4 μm, and the paraffin sections were dewaxed and further washed by distilled water. Lastly, the nucleus and cytoplasm were stained by hematoxylin and eosin, respectively.

2.3 Identification of NHE and NKA gene family members in *R. canadum*

For the complete identification of NHE and NKA gene family members in *R. canadum*, this study was based on the whole genome data of *R. canadum* (PRJNA634421) obtained in our laboratory and the NCBI public database, blast identification of NHE and NKA gene family members, recorded as the first round of screening results. The NHE and NKA gene family features were obtained from the Pfam database (http://pfam.xfam.org/) as PF00999 (Sodium/hydrogen exchanger family), PF00287 (Sodium/potassium ATPase beta chain), and PF00690 (Cation transporter/ATPase, N-terminus), respectively. The Hidden Markov Models (HMM) were used to obtain the features of the gene family. The HMMER 3.0 software was used to retrieve the whole-genome data, and the results of the second round of screening were tallied. Integrate the results, delete the mutilated or duplicate sequences and upload to SMART website and NCBI database for duplicate checks. The naming of NHE and NKA gene family members was based on reference comparisons and NCBI search results.

2.4 Structural analysis and genomic localization of the NHE and NKA gene families in *R. canadum*

In order to further investigate the NHE and NKA gene family members, we conducted several analyses. Firstly, we determined the intron and exon length information, as well as the genomic localization, based on the genome annotation file gff. Additionally,

we predicted the molecular weight (MW) and isoelectric point (PI) of the family members using the ExPasy website (http://web.expasy.org/). Moreover, we employed the MEME (Bailey et al., 2015) website (http://meme-suite.org/) to predict amino acid conserved motifs. Furthermore, we predicted the protein structural domains of NHE and NKA gene family members using the SMATR website. Finally, we utilized the TBtools software to map the NHE and NKA gene family structures and genomic localization.

2.5 Evolutionary analysis of the NHE and NKA gene families in *R. canadum*

The NHE and NKA family members from *Homo sapiens*, *Mus musculus*, zebrafish (*Danio rerio*), *S. maximus*, Rainbow Trout (*Oncorhynchus mykiss*), and *L. japonicus* were retrieved from the NCBI database. These sequences served as references for multiple amino acid sequence comparisons and homology analyses, which were performed using ClustalX1.83. The resulting phylogenetic tree was constructed by applying the neighbor-joining method (NJ) through MEGA-X (Kumar et al., 2016) software.

2.6 RNA-seq of NHE and NKA gene families in *R. canadum*

To investigate the impact of different salinity acclimation conditions on the expression patterns of NHE and NKA, RNA was extracted from the gills, intestine, and body kidney of *R. canadum* following 4 weeks of culture in salinities of 10‰, 30‰, and 35‰. RNA from nine fish in each salinity group was pooled to obtain one sample, and Illumina Hiseq^{TM}2000 was used to sequence the transcriptome. The raw mRNA sequencing data has been deposited in the NCBI Sequence Read Archive (SRA) under the accession number SRP202920 (published by our research groups) (Cao et al., 2020).

The raw mRNA sequencing data was processed using fastp (Chen et al., 2018) to remove low-quality data, and the remaining clean reads were mapped to the *R. canadum* genome (PRJNA634421) using HISAT2 software (Kim et al., 2015). StringTie software (Pertea et al., 2015) was then used to assemble the mapped reads. The expression of all genes in each sample (FPKM and reads count) was then calculated using RSEM (Li and Dewey, 2011), and the read count was normalized and analyzed for differentially expressed genes using edgeR (Robinson et al., 2010) ($P<0.05$ for significantly differentially expressed genes, FDR<0.05 and $|\log2FC|> 1$ for highly significant differentially expressed genes).The resulting expression data ($\log_2^{FPKM}$) were utilized to generate a gene expression heat map using TBtools, and correlation analysis was performed.

2.7 Analysis of qPCR expression of NHE and NKA genes in *R. canadum*

Gene-specific primers were designed based on the cDNA sequences for NHE and NKA gene family members, resulting in the amplification of fragments ranging from 100-230 bp (Table 1). β-actin was chosen as the reference gene. qRT-PCR was performed using a Roche Light Cycler^{TM} 96 real-time PCR machine and SYBR$^{®}$Select Master Mix. The expression levels of the three genes in 9 tissues and the expression levels of the genes in osmoregulatory organs such as gills, intestines, and kidneys after salinity adaptation were determined.

The amplification program consisted of an initial denaturation step at 95°C for 10 min followed by 40 cycles of denaturation at 95° C for 10 s, annealing at 60°C for 20 s, and extension at 72°C for 20 s. To minimize errors, three different *R. canadum* individuals were sampled for each salt treatment, and qPCR was repeated three times for each individual. The expression levels of *NHE1*, *NHE2a*, *NHE2c*, *NHE5*, *NKAα1b*, *NKAα3a*, *NKAβ1b*, and *NKAβ3a* genes were analyzed using the $2^{-\Delta\Delta Ct}$ method, and one-way ANOVA (LSD, Duncan) was performed using SPSS22.0 software.

3 Results

3.1 Analysis of organizational structure of *R. canadum* after salinity adaptation

After 30 days of domestication in low salinity water (10 ppt), the length (width) of gill filaments and gill lamellae of *R. canadum* increased significantly. The spacing between gill lamellae decreased, and the cells of gill lamellae were rounded and full. The number of chloride-secreting cells on gill filaments and gill lamellae decreased significantly. In the high salinity group (35 ppt), the number of chloride-secreting cells on gill filaments and gill lamellae increased slightly but not significantly. The width of gill filaments, gill lamellae, and cartilage tissues decreased significantly, and the spacing of gill lamellae increased (Figure 1A).

The microstructure of the intestine of juvenile *R. canadum* in the control group (30 ppt) showed that the single layer of columnar epithelium on the intestinal villi of juvenile *R. canadum* in the low salinity group became thicker, and the number of cupped cells decreased significantly. The size of the cupped cells did not change significantly. In the high-salinity group, the cytosol of the cup-shaped cells was enlarged, and the thickness of the unilamellar columnar epithelium and the number of cup-shaped cells on the intestinal villi did not change significantly (Figure 1B).

In the low salinity group, the tubular diameter of all levels of renal tubules of *R. canadum* increased, and the glomerulus was enlarged, full, and filled. The lumen of its capsule was small. In the high salinity group, the glomerulus atrophied, the lumen of the glomerular capsule increased, and the tubular diameter of all levels of renal tubules decreased slightly (Figure 1C).

3.2 Identification of NHE and NKA gene family members in *R. canadum*

In this study, the NHE and NKA families were characterized using genome–wide data and an HMM model. The analysis identified a total of 12 NHE family members and 12 NKA family

10.3389/fmars.2023.1228933

TABLE 1 Primers for qPCR of gene families.

Primer	Purpose	Sequence(5′-3′)	Length	GC%	Amplicon size
qNHE1-F	qRT-PCR	CCTGGGCACGATCCTGATGTTT	22	54.55	119
qNHE1-R	qRT-PCR	GTCCGTTGAGGTCTGATGGGTT	22	54.55	
qNHE2a-F	qRT-PCR	GCCATTGTTACCTGTGCCCT	20	55.00	168
qNHE2a-R	qRT-PCR	GTTCCACTCGTGCTCTGTTGTTA	23	47.83	
qNHE2b-F	qRT-PCR	CGCAGCAACACCAGCATCCAGTA	23	56.52	187
qNHE2b-R	qRT-PCR	CCACAGCCGTCAGCAACAGAACAC	24	58.33	
qNHE2c-F	qRT-PCR	TCCTCGACAGCGGCTACTTCAT	22	54.55	193
qNHE2c-R	qRT-PCR	ATGATGGCAGCGAACAGCAAGT	22	50.00	
qNHE3 -F	qRT-PCR	GTAGCCGTCATCGCCGTGT	19	63.16	100
q NHE3 -R	qRT-PCR	GCACCACTGTCACACCATCGT	21	57.14	
qNHE5-F	qRT-PCR	TTGCTCTGGTGGTGCTGCTG	20	60.00	166
qNHE5-R	qRT-PCR	ATGGTCGGCTTCCTGCTGGT	20	60.00	
qNHE6a-F	qRT-PCR	TGGACCTGTACGCTCTGCTGTT	22	54.55	101
qNHE6a-R	qRT-PCR	GTTGTCTCCTTCTGGCTGGTATGC	24	54.17	
qNHE6b-F	qRT-PCR	TGGATGGGTCACAGAGAAGGAACA	24	50.00	141
qNHE6b-R	qRT-PCR	CACAACAAGCAGGCAGAGTAGCA	23	52.17	
qNHE7-F	qRT-PCR	CTACCGAGAAGGAGGCAGAGGAA	23	56.52	167
qNHE7-R	qRT-PCR	ACCCACCAGCAAACCGTAAATCAT	24	45.83	
qNHE8-F	qRT-PCR	GAGATGACGACGGAGGAGAGGTGAA	25	56.00	171
qNHE8-R	qRT-PCR	CAGCAGGTGTTGTAGAGTGGATGGT	25	52.00	
qNHE9-F	qRT-PCR	ACTCTGCTGCTGGTCTGCTTCA	22	54.55	153
qNHE9-R	qRT-PCR	TGTTGTGTCCTGCCTCCCTGTA	22	54.55	
qNHEβ-F	qRT-PCR	TCCGCTGAGGTCTTCCATCTGT	22	54.55	141
qNHEβ-R	qRT-PCR	GCTCACGCTGCTCCACATCTTC	22	64.02	
qNKAα1a-F	qRT-PCR	GCTGTCATCTTCCTCATCGGTATCA	25	48.00	123
qNKAα1a-R	qRT-PCR	GTTCTTCACCAGGCAGTTCTTCTTG	25	48.00	
qNKAα1b-F	qRT-PCR	TCGTCATCATCACTGGTTGCTTCTC	25	48.00	177
qNKAα1b-R	qRT-PCR	TGTCTCCACCTTTCACCTCCACTAA	25	48.00	
qNKAα2-F	qRT-PCR	GCATACACACTAACCAGCAACATCC	25	48.00	152
qNKAα2-R	qRT-PCR	GCCGCCTCGTAAGCCAATGA	20	60.00	
qNKAα3a-F	qRT-PCR	GGTGATGGTGTGAACGACTCTCC	23	56.62	149
qNKAα3a-R	qRT-PCR	CCTTCTTCTACTCCTGTGACGATGG	25	52.00	
qNKAα3b-F	qRT-PCR	TCTCAGGCTCCGATGTGTCCAA	22	54.55	196
qNKAα3b-R	qRT-PCR	GGCAGAGGAATGTTGACGATGATGA	25	48.00	
qNKAβ1a-F	qRT-PCR	ACGTGATATTCTACGGATGCTTGG	24	45.83	101
qNKAβ1a-R	qRT-PCR	GACTCTGTCCTGATAGGTGGGTTT	24	50.00	
qNKAβ1b-F	qRT-PCR	GTCTGACACACACCCCACGCT	21	61.99	140
qNKAβ1b-R	qRT-PCR	CTTCATCTGGTCCCTCTGGTTCTC	24	54.17	
qNKAβ2a-F	qRT-PCR	TGTGGAGCCAAGAGTTACAAAGTG	24	45.83	123

(Continued)

TABLE 1 Continued

Primer	Purpose	Sequence(5′-3′)	Length	GC%	Amplicon size
qNKAβ2a-R	qRT-PCR	GCCGTAGTATGGGTAGTACATGAGAT	26	46.15	
qNKAβ2b-F	qRT-PCR	ACTTCAAGCAGGATGACAGCG	21	52.38	206
qNKAβ2b-R	qRT-PCR	ACCACAGGTGACATACGGAGC	21	57.14	
qNKAβ3a-F	qRT-PCR	CGTCTGAAGGTCGGCTGGATAA	22	54.55	136
qNKAβ3a-R	qRT-PCR	CACTCCACCGTCTGCTCAATGT	22	54.55	
qNKAβ3b-F	qRT-PCR	TGTTGCTGCTCACTCTGGATG	21	52.38	192
qNKAβ3b-R	qRT-PCR	CCTCGTTCTTCTCCTGCTCTGTATC	25	52.00	
qNKAβ4-F	qRT-PCR	ATGACATCGCCTTTAACGCCTCTG	24	50.00	181
qNKAβ4-R	qRT-PCR	AACTGACACGCTTTCCGCTCTG	22	54.55	
β-actin-F	qRT-PCR	AGGGAAATTGTGCGTGAC	18	50.00	114
β-actin-R	qRT-PCR	AGGCAGCTCGTAGCTCTT	18	55.56	

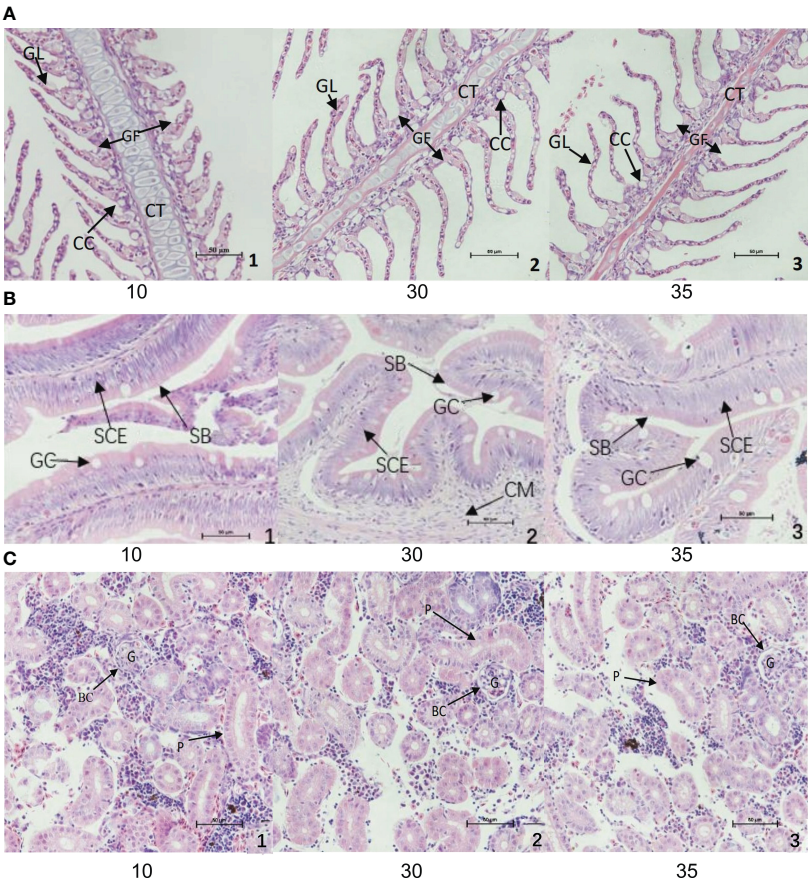

FIGURE 1
Structural changes of gill **(A)**, intestine **(B)** and body kidney **(C)** of juvenile of *R. canadum*. 10, salinity 10 ‰; 30, salinity 30 ‰; 35, salinity 35 ‰. GF, gill filaments; GL, gill small pieces; CC, chlorinated cells; CT, cartilage tissue; SCE, monolayer columnar epithelium; SB, striatum; GC, goblet cells; CM, ring muscle; G, glomerulus; BC, renal capsule; P, renal tubule.

members, including both single-copy and multi-copy genes. Specifically, *NHE2* and *NHE6* were found to be multi-copy genes, while *NKA1*, *NKA3*, and *NKAβ1~3* were also identified as multi-copy genes. The coding sequence (CDS) of NHE genes ranged from 1818 to 2940 bp in length, with amino acid sizes ranging from 606 to 980 aa. The PI ranged from 5.5 to 9.45, and the Mw ranged from 67.04 kD to 107.53 kD. Similarly, the CDS of NKA genes ranged from 837 to 3099 bp in length, with amino acid sizes ranging from 279 to 1033 aa. The PI ranged from 5.01 to 8.09, and the Mw ranged from 32.67 kD to 113.47 kD (Table 2).

3.3 Structural analysis and genomic localization of the NHE and NKA gene families in *R. canadum*

The NHE family members of *R. canadum* had 2 to 16 Coding DNA Sequence (CDS), with *NHE3*, *NHE7*, *NHE8*, and *NHE9* having 16 CDS, and *NHEβ* having the least number of CDS with only 2, which might be attributed to genome assembly issues. In contrast, *NHE1* had the highest number of CDS with 15 (Figure 2A). The number of CDS of NKA family members ranged from 5 to 23, with *NKAα* members and *NKAβ* members showing polarized CDS numbers, where none of the former had less than 21 and all of the latter had less than 10 CDS, implying a correlation between CDS numbers and subtype classification (Figure 2B).

The present study aimed to analyze the motif composition of NHE and NKA genes in *R. canadum* using the MEME website. The results showed that both gene families contained 10 motifs arranged in an organized and regular manner. Most motifs of NHE genes were associated with Na^+/H^+ exchanger structural domains, except for motif4, while all motifs identified in NKA were associated with Cation transporter/ATPase and Hydrolase structural domains. Further analysis revealed that NHE motif1 and motif4 were mainly identified in *NHE1~5*, and motif 8 appeared only twice in *NHE8* and once in all other members. In contrast, motif4 appeared in the anterior segment of the *NHE9* sequence. Furthermore, *NHEβ* lacked motif7 and had more motif10 compared to *NHE1* (Figure 3A). Concerning the NKA gene family, motif10 was found only in the *NKAβ* isoform, while the remaining nine motifs were ordered in the *NKAα* isoform (Figure 3B). The only difference was that motif4 was missing in *NKAα1b*.

The domain information of NHE and NKA genes in *R. canadum* was predicted using the SMART website, which revealed that NHE genes contained CPA1 and NHE structural domains (Figure 3C), and NKA genes contained NKA and CPA-N/C structural domains (Figure 3D).

Genomic localization shows that members of the NHE and NKA gene families of *R. canadum* localize to 10 and 9 superscaffolds, respectively (Figure 4). Specifically, *NHE2b* and *NHE6a* were present simultaneously on superscaffold16 and superscaffold3, respectively, while the remaining eight members of NHE family were distributed randomly on a single superscaffold (Figure 4A). Similarly, 2-3 members of NKA family (*NKAβ1b*, *NKAα1b*, and *NKAα1a*; *NKAα2* and *NKAβ3*) were simultaneously present on superscaffold24 and superscaffold14, respectively. In contrast, the remaining eight members of NKA family were randomly distributed on a single superscaffold (Figure 4B). Moreover, the multi-copy members of NHE family, *NHE2a-c*, were localized to the 9th, 3rd, and 24th superscaffold, respectively, whereas *NHE6a* and *NHE6b* were localized to the 3rd and 12th superscaffold, respectively (Figure 4A) multi-copy. Additionally, the multi-copy members of NKA family, *NKAβ1-3* and *NKAα3a* and *NKAα3b*, were identified in the 7th, 24th, 23rd, 12th, 5th, and 14th superscaffold, respectively, and *NKAα1a* and NKAα1b were localized in both superscaffold 24 (Figure 4B).

TABLE 2 Sequence characteristic of *NHE* and *NKA* gene families.

Gene	PI	Mw/Da	CDS/bp	Length/aa	Location	Accession numbers
NHE1	8.3	89.77	2436	812	Superscaffold 4	OR095067
NHE2a	9.45	98.21	2622	874	Superscaffold 9	OR095068
NHE2b	9.15	75.12	2004	668	Superscaffold 3	OR095069
NHE2c	8.2	94.10	2514	838	Superscaffold 24	OR095070
NHE3	5.95	100.84	2718	906	Superscaffold 16	OR095071
NHE5	8.32	107.53	2940	980	Superscaffold 1	OR095072
NHE6a	5.61	77.32	2079	693	Superscaffold 3	OR095073
NHE6b	6.29	77.73	2118	706	Superscaffold 12	OR095074
NHE7	5.96	77.28	2091	697	Superscaffold 7	OR095075
NHE8	5.72	72.70	1950	650	Superscaffold 6	OR095076
NHE9	5.5	67.04	1818	606	Superscaffold 20	OR095077
NHEβ	8.75	84.83	2295	765	Superscaffold 16	OR095078
NKAα1a	5.23	112.50	3075	1024	Superscaffold 7	OR095079
NKAα1b	5.19	113.47	3099	1033	Superscaffold 24	OR095080
NKAα2	5.3	111.36	3033	1011	Superscaffold 14	OR095081
NKAα3a	5.27	112.73	3069	1023	Superscaffold 5	OR095082
NKAα3b	5.25	111.30	3033	1011	Superscaffold 4	OR095083
NKAβ1a	8.02	34.85	906	302	Superscaffold 24	OR095084
NKAβ1b	6.24	34.42	906	302	Superscaffold 24	OR095085
NKAβ2a	8.09	34.21	894	298	Superscaffold 23	OR095086
NKAβ2b	6.84	35.37	918	306	Superscaffold 12	OR095087
NKAβ3a	5.01	38.73	996	332	Superscaffold 16	OR095088
NKAβ3b	7.51	32.67	837	279	Superscaffold 14	OR095089
NKAβ4	7.61	39.36	1029	343	Superscaffold 3	OR095090

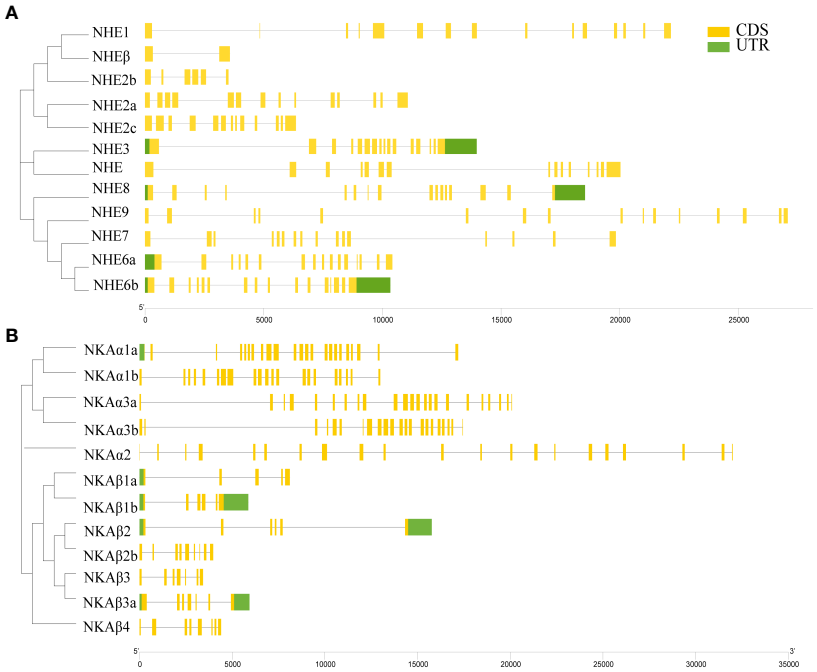

FIGURE 2
Gene structure of NHE **(A)** and NKA **(B)** gene families.

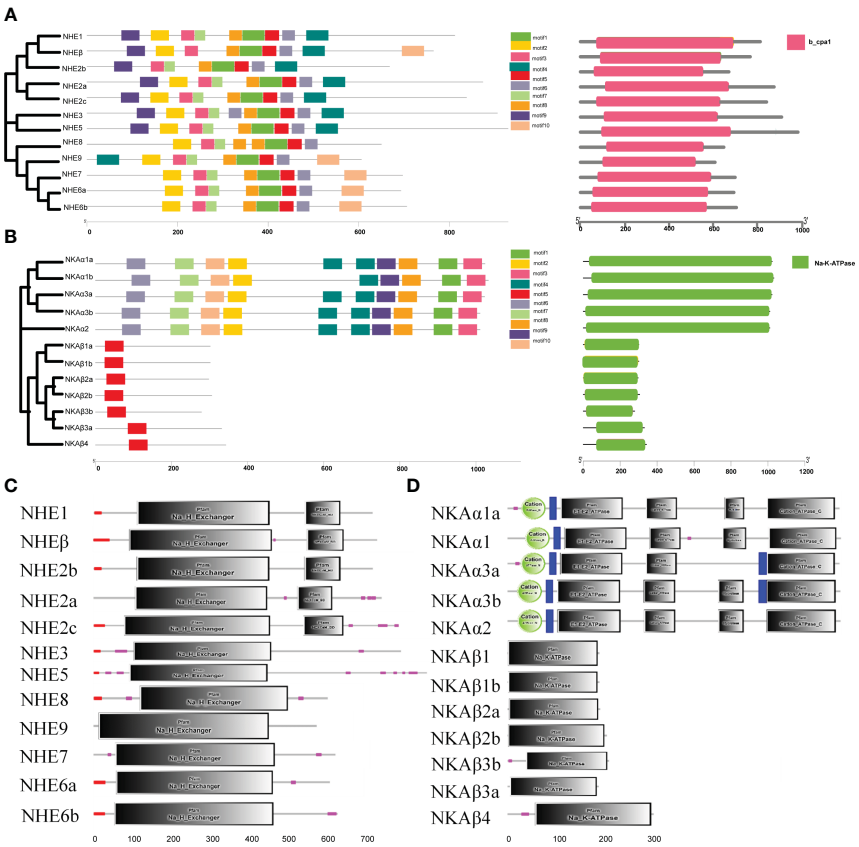

FIGURE 3
Motif of NHE **(A)** and NKA **(B)** gene families and domain of *NHE* **(C)** and *NKA* **(D)** gene families.

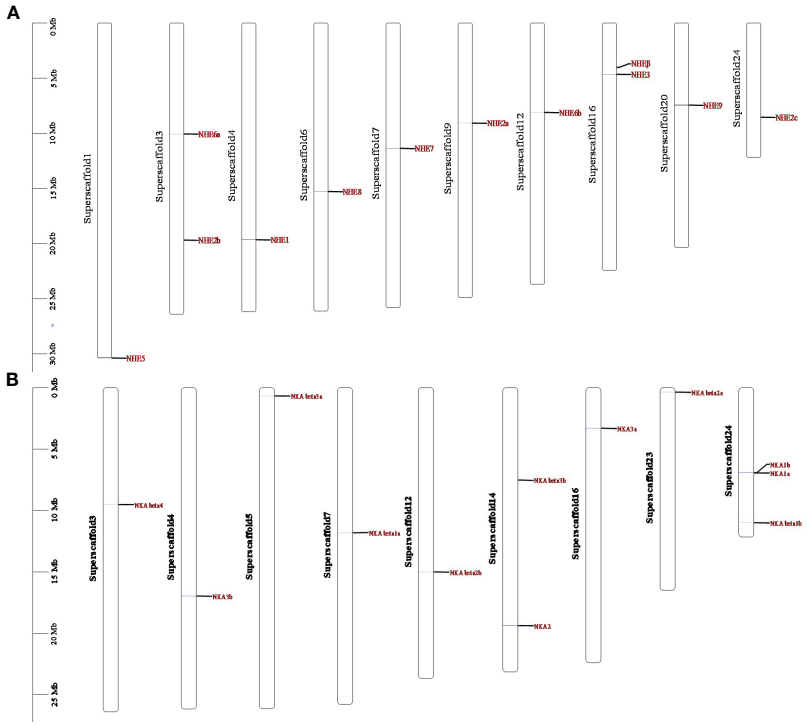

FIGURE 4
Genomic mapping of NHE **(A)** and NKA **(B)** gene families.

3.4 Phylogenetic analysis of the NHE and NKA gene families in *R. canadum*

The NHE and NKA gene family members of six species, including *Homo sapiens*, *Mus musculus*, *D. rerio*, *S. maximus*, *O. mykiss*, and *Lateolabrax maculatus*, were used as references to construct a phylogenetic evolutionary tree, which further verified the accuracy of the annotation of the NHE and NKA genes of *R. canadum* and revealed the variation of these genes during species evolution (Figure 5). The analysis indicated that *NHE1~9* of *R. canadum* were most closely related to teleost and furthest from mammals. *NHE1* and *NHEβ* were clustered into a single clade with teleost such as *D. rerio* and *S. maximus*, respectively, before merging into one clade; *NHE3* and *NHE5* of *R. canadum* were merged into one clade, while *H. sapiens* and *M. musculus* were separate clades. The multi-copy genes *NHE2a~c* were clustered with other species and re-clustered with mammalian *NHE4*, respectively; *NHE6a* and *NHE6b* were alone, and their closest relatives were *L. japonicus*, *S. maximus*, *D. rerio* and *O. mykiss* (Figure 5A). Additionally, the *NKAα* subtype gene and *NKAβ* subtype gene of *R. canadum* were separately divided into the same branch with other species and were most closely located with teleost. Among them, *NKAα4* of *H. sapiens* and *M. musculus* were separately merged with *NKAβ1a* of *R. canadum*. Moreover, *NKAα1a~b* and *NKAα2* of *R. canadum* were closest together and merged into one branch, and *NKAα1* and *NKAα2* of *H. sapiens* and *M. musculus* were independently into one branch (Figure 5B).

3.5 Analysis of the expression patterns of NHE and NKA gene families in *R. canadum*

To investigate the expression patterns of the NHE and NKA gene families in various tissues of *R. canadum* under normal seawater salinity, qRT-PCR was used to determine the gene expression abundance in nine different tissues. The results demonstrated that the NHE and NKA family members of *R. canadum* were widely expressed in all tissues, including the gill, brain, heart, intestine, kidney, liver, spleen, stomach and muscle (Figure 6). Specifically, the tissues with high expression of NHE were the gill, somatic kidney, and brain, while NKA was highly expressed in the gill, brain, and heart.

Of the single-copy genes, *NHE1* and *NHE3* showed similar expression patterns and were mainly concentrated in the gill and somatic kidney. On the other hand, *NHE5* and *NHE7* were highly expressed in the liver and brain, respectively. The highest expression signals of multi-copy genes *NHE2a* and *NHE2b* were detected in the brain and muscle, respectively, while the highest expression tissues were the gill and liver for *NHE6a*, and the somatic kidney and brain for *NHE6b* multi-copy. Furthermore, *NHEβ* and *NHE1* expression patterns were inconsistent, with high expression detected only in the brain and trace expression in other tissues (Figure 6A).

The NKA family members *NKAα1a*, *NKAβ1b*, *NKAβ2a*, and *NKAβ3a* were highly expressed in osmolarity-regulating organs, such as the gill, intestine, and somatic kidney, respectively. Among

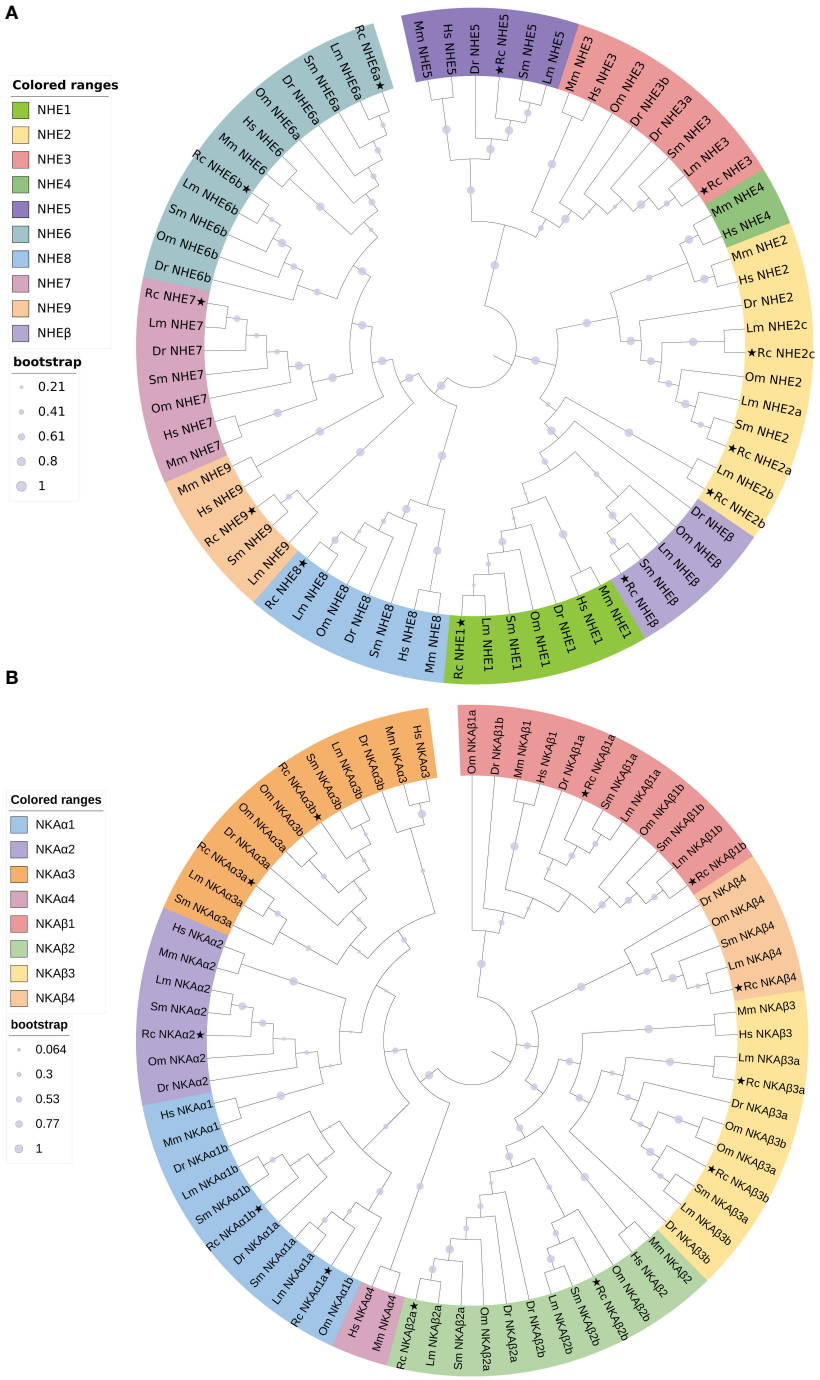

FIGURE 5
Phylogenetic analysis trees of *R. canadum* NHE **(A)** and NKA **(B)** gene families. Rc, *R. canadum*; Dr, *D. rerio*; Sm, *S. maximus*; Lm, *L. maculatus*; Hs, *H. sapiens*; Mm, *M. musculus*.

them, *NKAα1a* was the most highly expressed in the gill. *NKAα2* was expressed only in the brain and muscle, while *NKAβ4* was highly expressed in the brain, with lower expression levels in other tissues. Most of the multi-copy genes (*NKAα1b*, *NKAα3a*, *NKAα3b*, *NKAβ1a*, *NKAβ2a*, *NKAβ2b*, *NKAβ3a*, and *NKAβ3b*) were highly expressed in brain tissues, with *NKAα1b* only detected as a fluorescent signal in brain tissues, not consistent with *NKAα1a*. *NKAα3a* and *NKAα3b* showed similar expression patterns, with high expression in the brain, heart, somatic kidney, and gill in descending order. *NKAβ1a* was highly expressed in several tissues, mainly in the brain, stomach, and muscle, while *NKAβ1b* was highly expressed mainly in the somatic kidney. *NKAβ2a* was highly expressed in the gill, intestine, brain, stomach, and muscle, while *NKAβ2b* was hardly expressed except in the brain and muscle. The expression pattern difference of *NKAβ3a-NKAβ3b* was similar to that of *NKAβ2a-NKAβ2b*. Additionally, fluorescent signals of other

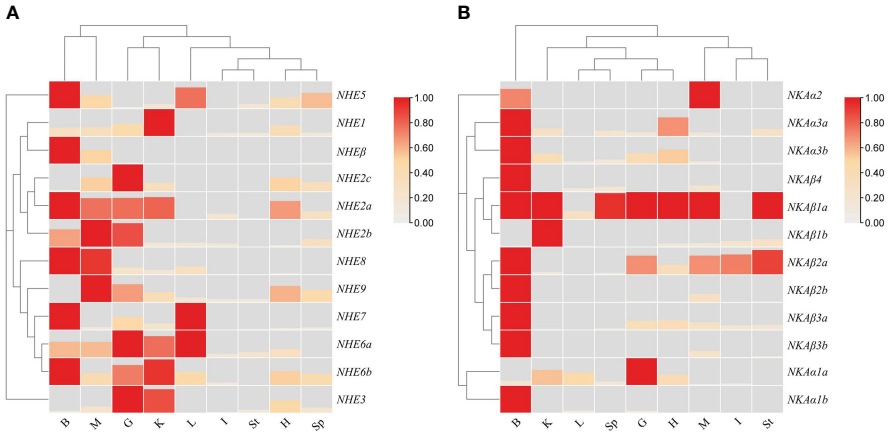

FIGURE 6
Heat map of tissue expression of NHEs **(A)** and NKAs **(B)** in *R. canadum*. G, gill; I:intestine; K,Kidney; L, Liver; H, Heart; B, Brain; Sp, Spleen; St, Stomach; M, Muscle.

members were less frequently detected in the liver, spleen, and stomach, except for *NKAα1a*, *NKAβ1a*, and *NKAβ2a*, which showed expression (Figure 6B).

3.6 Transcriptome analysis of the NHE and NKA gene families in *R. canadum*

The effects of salinity acclimation on the expression patterns of NHE and NKA gene families in different tissues of *R. canadum* was investigated using a reference transcriptome sequencing approach and validated by qRT-PCR. The results demonstrated that the expression patterns of NHE and NKA genes were influenced by salinity and exhibited tissue-specific characteristics (Figure 7). In gill tissues, the expression of *NHE3* was significantly down-regulated under salinity 10 and 35 acclimation conditions compared to the control group acclimated at salinity 30. Additionally, *NHE6b* and *NHE8* were significantly down-regulated under salinity 35 acclimation conditions, while *NHE2a* was significantly down-regulated under salinity 10 acclimation conditions. However, the experimental group exhibited significant upregulation in *NHE2c* expression, and *NHE7* showed significant upregulation under salinity 35 acclimation conditions. In intestinal tissues, the expression levels of NHE genes were significantly increased under experimental conditions (salinity 10 and 35) compared to the salinity 30 control. Specifically, *NHE7* was significantly upregulated under both low (10) and high (35) salinity acclimation conditions, while *NHE1* and *NHE6a-b* were only significantly upregulated under salinity 35 acclimation conditions. *NHE9* exhibited significant upregulation under salinity 10 acclimation conditions. In kidney tissues, *NHE3* expression increased with higher salinity and showed highly significant upregulation at salinity 35, along with significant downregulation at salinity 10 compared to the salinity 30 control. *NHE6a* exhibited significant upregulation at salinity 35, whereas *NHE2a* showed significant downregulation at salinity 10. *NHE5* and *NHEβ* expression levels remained relatively stable across all three salinity acclimation conditions in all tissues, while *NHE2b* and *NHE5* expression levels were comparatively low under all conditions (Figure 7A).

In gill tissues, *NKAα3a*, *NKAα3b*, and *NKAβ1a* expression levels were significantly upregulated under salinity acclimation conditions of 10 and 35, with *NKAα3a* displaying particularly highly significant upregulation at salinity 10 compared to the control group at salinity 30. Conversely, *NKAα1b* expression was significantly downregulated at both salinities 10 and 35. In gill, intestinal, and kidney tissues, the expression levels of *NKAα1a* and *NKAβ1b* showed significant increases with increasing salinity. In intestinal tissues, *NKAβ2a* and *NKAβ4* expression levels were significantly upregulated at salinity acclimation condition of 10, and exhibited highly significant upregulation at salinity acclimation condition of 35. Additionally, *NKAα1b*, *NKAα3b*, *NKAβ1a*, and *NKAβ3a* were significantly upregulated at salinity acclimation condition of 35 compared to the control. In kidney tissues, *NKAβ1a* expression was significantly downregulated at salinity 35, while *NKAα3b* showed significant upregulation at salinity 10 compared to the control group. However, the expression levels of *NKAα2*, *NKAα3a*, and *NKAβ2b* were relatively low under all conditions (Figure 7B). The qRT-PCR validation and RNA-seq were in general agreement in terms of the fold change in differential expression (Figure 7C). In the linear regression analysis of trend changes, $R^2 = 0.8959$ (Figure 7D). The results indicate that the gene expression analysis based on RNA-Seq data is reliable.

3.7 Salinity-adapted qPCR expression analysis of the NHE and NKA gene families of *R. canadum*

To investigate the differences in the expression patterns of some members of the NHE and NKA gene families of *R. canadum* under salinity acclimation, qPCR was performed on *R. canadum* acclimated to salinities of 10‰, 30‰ and 35‰ for 4 weeks in this study. The results showed that the relative expression of *NHE1*

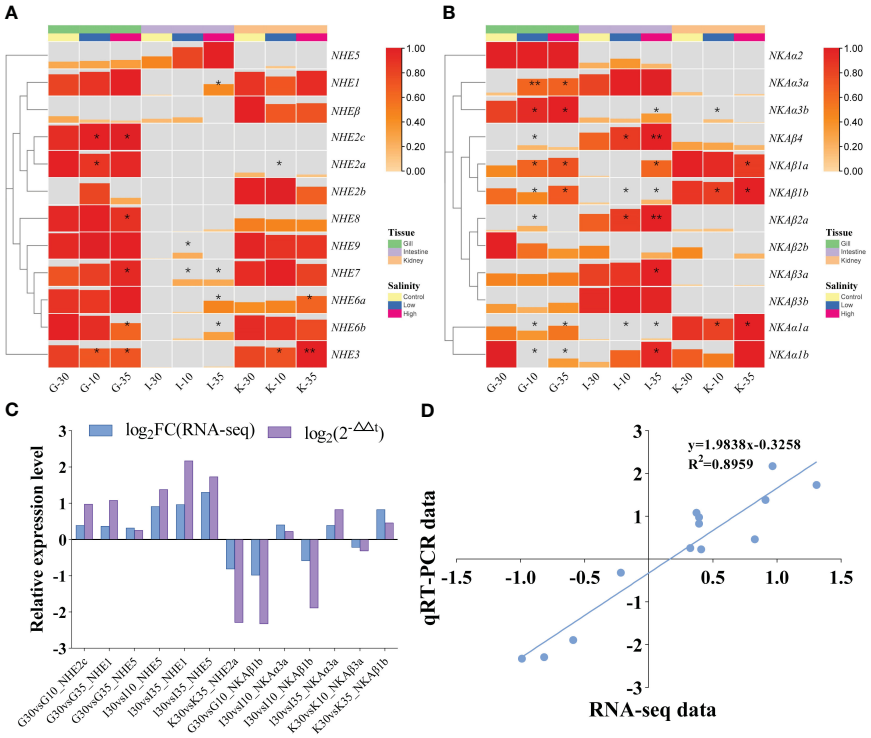

FIGURE 7
Transcriptome expression patterns of NHEs **(A)** and NKAs **(B)** of *R. canadum* under different salinity acclimation. Relative expression level **(C)** and linear regression **(D)** of RNA-Seq and qRT-PCR data that are expressed as a $\log_2$ fold change. 10, salinity 10 ‰; 30, salinity 30 ‰; 35, salinity 35 ‰; G, gill; I, intestine; K, kidney.

was significantly up-regulated in the intestine and down-regulated in the kidney after increasing or decreasing salinity, while the expression was not significantly increased in the gills after decreasing salinity (Figure 8A). In addition, *NHE2a* expression in the gill did not change significantly in low-salt acclimation, while it was significantly down-regulated in high-salt acclimation (Figure 8B). *NHE2c* was significantly down-regulated in gill, intestine and somatic kidney with increasing salinity (Figure 8C), and *NHE5* was also significantly down-regulated in somatic kidney. In addition, the expression pattern of *NHE5* in both gill and intestine was significantly different in a "U" pattern (Figure 8D).

Following low-salt acclimation, significant down-regulation of *NKAα1b* and *NKAβ3a* was observed in the gills of *R. canadum* (Figures 8E, H), while *NKAα3a* and *NKAβ1b* did not exhibit significant changes (Figures 8F, G). In the intestine, *NKAα1b* and *NKAβ1b* did not exhibit significant changes (Figures 8E, G), whereas *NKAα3a* and *NKAβ3a* were significantly up-regulated and down-regulated, respectively (Figures 8F, H). In the somatic kidney, *NKAα1b*, *NKAα3a*, and *NKAβ3a* showed significant up-regulation (Figures 8E, F, H), while *NKAβ1b* did not change significantly (Figure 8G). Upon high-salt acclimation, the expression of *NKAα1b* and *NKAβ3a* in the gills remained consistent with low-salt acclimation (Figures 8E, H), while *NKAα3a* and *NKAβ1b* exhibited significant up-regulation (Figures 8F, G). In the intestine, the expression levels of *NKAα1b*, *NKAα3a*, and *NKAβ1b* were significantly increased (Figures 8E, F, G), while *NKAβ3a* expression levels were significantly decreased (Figure 8H). The expression pattern of *NKAα3a* and *NKAβ3a* in the somatic kidney was consistent with low-salt adaptation (Figures 8F, H), while *NKAα1b* and *NKAβ1b* expression were unaffected by salinity (Figures 8E, G).

4 Discussions

The process of salinity adaptation in fish can be divided into two stages: passive adaptation to the external environment and active osmoregulation (Li et al., 2022). The key to salinity adaptation in fish is ion transport, and this regulation is primarily performed by osmoregulatory organs such as the gills, kidneys, and intestines (Whittamore, 2012; Dawood et al., 2021; Ali et al., 2022). The gills are the major organ of osmoregulation in fish and play an important role in maintaining the balance between the internal and external environment of the fish, which is closely related to the ion transport gene sodium/potassium pump (NKA) on the cell membrane (Dawood et al., 2021). In this study, the gill filaments and gill lamellae of juvenile *R. canadum* in the low salinity group were more round and full, and wider than those in the control group. On *L. japonicus*, *Acipenser schrenckii* and *Gymnocypris przewalskii*, gill tissues underwent similar adaptive changes in order to maintain osmoregulatory homeostasis (Hou et al., 2006; Wang and Hu, 2009; Huang et al., 2022). This is because the gill filaments and gill lamellae of juvenile fish living in a desalinated environment tend to change to wider and longer to facilitate sufficient contact with the water column

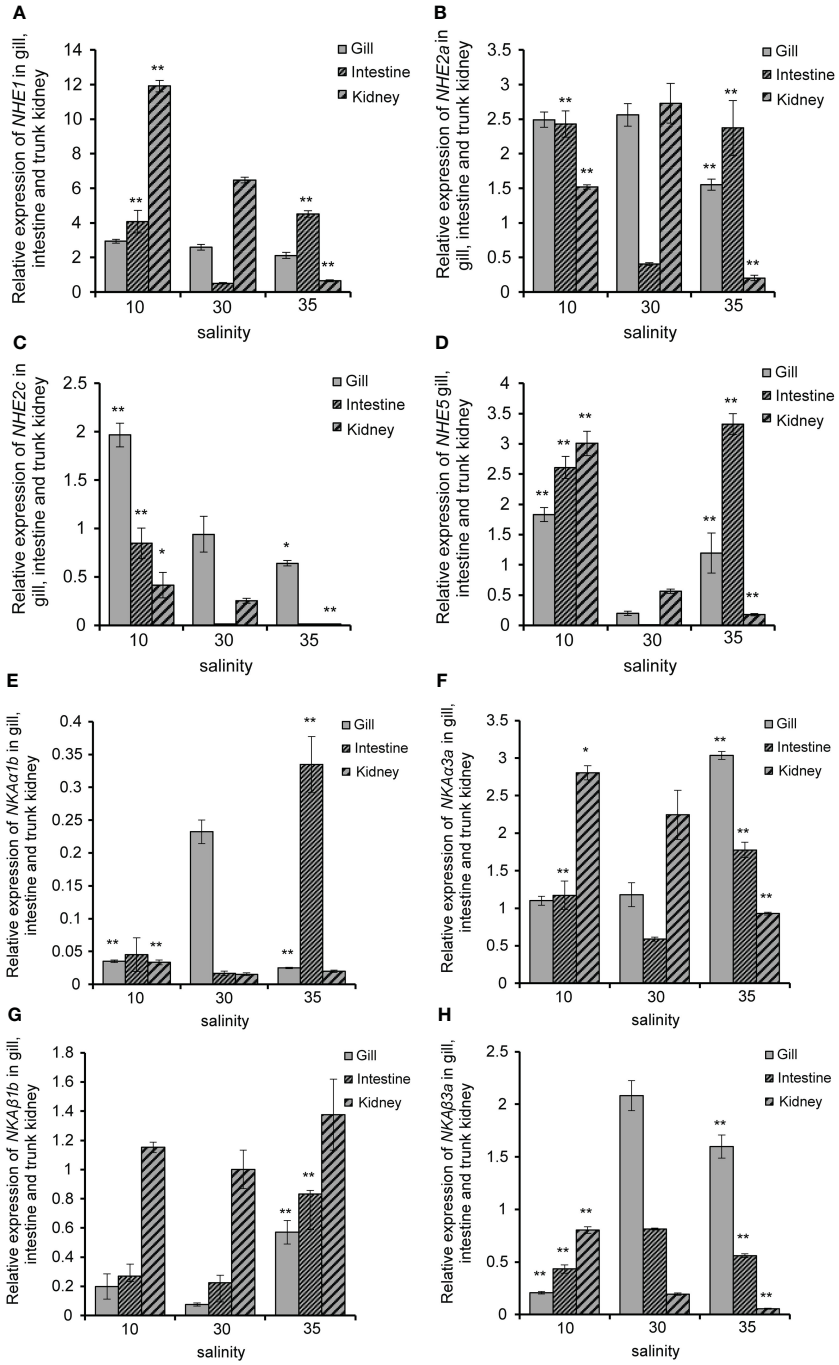

FIGURE 8
Relative expression of *R. canadum NHE1* **(A)**, *NHE2a* **(B)**, *NHE2* **(C)**, *NHE5* **(D)**, *NKAα1b* **(E)**, *NKAα3a* **(F)**, *NKAβ1b* **(G)** *and NKAβ3a* **(H)** in different tissue after salinity adaption. 10, salinity 10 ‰; 30, salinity 30 ‰; 35, salinity 35 ‰. * and* * indicated that the expression of each gene was significantly different from that of the control group, and the significance levels were $P < 0.05,0.01$, respectively.

and thus take up inorganic ions in the water to adapt to the hypotonic environment (Yu et al., 2012; Li et al., 2014). Conversely, gill filament cells shrank, and gill lamellae spacing increased at high salinity. These changes increased water and oxygen exchange between the fish and the external environment, which promoted better survival of fish under high salinity conditions (Yang et al., 2014). In this experiment, the number of chloride-secreting cells in *R. canadum* decreased at low salinity and increased at high salinity. Chloride-secreting cells are important regulatory cells that adapt to different salinities in euryhaline fish, and they have abundant Na^+/K^+-ATPase on the microtubule system in their cytoplasm (Sakamoto et al., 2001). During salinity changes, chloride-secreting cells secrete Cl^- in hypotonic regulation and absorb Na^+ and Cl^- in hypertonic regulation to regulate osmotic pressure homeostasis (Foskett et al., 1983; Marshall, 2011). This shows that the gills of *R. canadum* have certain adaptability when the external salinity changes.

The intestine of fish plays a smaller role in osmoregulation, but it has slao been shown that the intestinal epithelial cell membrane can be involved in active transmembrane transport of Na^+, K^+ and Cl^- inside and outside the cell through ion channel transporter proteins, combined with passive transport of water to maintain osmotic pressure homeostasis in the body (Li et al., 2011). In our study, we observed changes in the intestinal villi structure of juvenile *R. canadum* in the low salinity group, where the monolayer columnar epithelium of intestinal villi became thicker. These results are consistent with the speculation of Sun et al. (2016). who hypothesized that low salinity has a detrimental effect on the intestine of *Takifugu rubripes*. We also observed changes in cupped cells, which secrete mucus to lubricate the epithelial surface and remove waste (Kibenge and Strange, 2021). The number of cupped cells decreased at low salinity, while the cytosol of cupped cells became larger at high salinity. Further research is necessary to determine whether these changes in cupped cells are related to salinity adaptation in juvenile *R. canadum*. The kidney is another important organ in the regulation of osmotic pressure in fish, as the glomerulus filters blood cells and macromolecular proteins from the blood, and the renal tubules reabsorb water, glucose and amino acids (Smith, 1932; Gonzalez, 2012). In this study, the tubular diameter of all levels of renal tubules in the low-salinity group became larger, the glomeruli were expanded, full and filled, and the gap in the inner wall of the renal capsule was reduced; in the high-salinity group, the glomeruli were atrophied and the gap in the inner wall of the renal capsule was increased. This structural change was beneficial to the filtration and reabsorption of nutrients in the blood of juvenile *R. canadum*.

Changes in water salinity have a significant impact on the osmotic pressure of fish organisms, and fish have developed various mechanisms to counteract the negative effects of salinity by activating activities such as their own water-salt regulation (Gonzalez, 2012). Sodium hydrogen exchanger (NHE) is a class of ion channel proteins present in most species, involved in the intracellular and extracellular transport of Na^+ and H^+ ions, and plays a critical role in cellular acid-base homeostasis, cell volume regulation, and osmotic pressure regulatory networks in fish, such as Na+ reabsorption in the kidney, stomach, and intestine (Edwards et al., 2005). *NHE3*, one of the NHE family members, also forms an ion regulatory network in teleost with NKA, *NKCC1*, NCC, and CFTR, which together maintain salt secretion and ion transport of Na^+, K^+, and Cl^- in and out of the membrane (Marshall, 2011). Current studies in fish osmoregulation have focused on *NHE2* and *NHE3*. For example, Yan et al. (2007) reported that *D. rerio* treated with soft water had increased expression of *DrNHE2* and *DrNHE3* genes in the gills and were enriched in mitochondrion-rich cells (MRCs). The gill of *LjNHE3* expression level of *L. japonicus* was upregulated after low salt stress (Inokuchi et al., 2017). The number of *NHE* family members varies somewhat among species; for instance, *NHEβ4* is identified in mammals such as *H. sapiens* and *M. musculus*, but not in teleost such as *D. rerio*, *Oryzias latipes*, and *Dicentrarchus labrax* (Tine et al., 2014). Sodium/potassium-transporting ATPase (NKA), the main active pump in the gill, is responsible for Na^+ ion transport as well as NHE, except that it empowers the ion transport system of multiple osmolarity-regulated epithelial cells by hydrolyzing ATP (Lin et al., 2003). It is now known that in teleosts, NKA exists in both α and β subunits and is classified as such (Zhang et al., 2019). Among them, the former is responsible for adenosine triphosphatase catalysis and Na^+ and K^+ transport activities, while the latter is mainly responsible for auxiliary α-subunit folding (Sundh et al., 2014). A variety of *NKAα* isoforms are expressed in fish osmoregulatory organs, and their expression levels are positively or negatively correlated with salinity changes, indicating that different NKA isoforms are involved in osmoregulatory processes and have different roles (Yang et al., 2016; Hu et al., 2017).Further studies on the NHE and NKA gene families may provide insights into the potential functions of the remaining members and enhance our understanding of osmoregulation in fish.

A total of 12 NHE genes and 12 NKA genes were identified in *R. canadum*. These genes were found to be distributed randomly on 10 and 9 superscaffolds, respectively, which is consistent with the findings reported by Zhang et al. (2019). The gene sequences of NHE and NKA gene family members were compared with those of *O. mykiss*, *L. japonicus* and *S. maximus* to name them and analyze the conserved motifs and structural domain characteristics (Berthelot et al., 2014; Figueras et al., 2016; Gao et al., 2022). The results revealed that the motifs and domains of the NHE genes were concentrated in the Na^+/H^+ exchanger domains, which the identification of the NKA also showed that they closely association with Cation transporter/ATPase and Hydrolase domains, and the motifs and domains of different members were arranged in different patterns. This indicates that the sequence characteristics of NHE and NKA members are closely related to their taxonomy and functions. In other teleost fishes, *NHE4* is commonly missing and *NHEβ* is only found in teleost fishes (Kasahara et al., 2007; Howe et al., 2013; Tine et al., 2014). In this study, *NHE4* was lost but *NHEβ* was identified by phylogenetic analysis. The results shown that NHE and NKA genes were the closest to teleosts in taxonomic status and the farthest from mammals, indicating that the protein sequences of the two family members were highly conserved in species evolution. The results of qRT-PCR showed that NHE and NKA family members were widely distributed in nine tissues such as heart, liver and spleen, and the expression patterns of NHE multi-copy gene members were different, such as *NHE2a* and *NHE2b* high expression tissues. However, the expression patterns of NKA multi-copy gene members are partially similar, all of which are highly expressed in brain tissue, but *NKAβ1a* and *NKAβ1b* are highly expressed in stomach, muscle and body kidney, respectively. There are significant differences between the two, indicating that multi-copy genes are functionally different.

The expression patterns of NHE and NKA gene families in *R. canadum* differed significantly in different salinities. Significant up-regulation of gill *NHE2c* and *NHE5* expression in *R. canadum* occurred after low-salt acclimation, while no significant changes were found in *NHE2a*, and similar results were found in *L. maculatus*, suggesting that *NHE2c* and *NHE5* may play an important role in the gill tissue of *R. canadum* in low-salt acclimation (Zhang et al., 2019). Studies have reported that *NHE1* expression trends in *S. maximus* gill, intestine and somatic kidney

were negatively correlated with salinity changes and showed low salt adaptation (Zhang et al., 2020). In the present study, significant upregulation of *NHE1* in the intestine and somatic kidney of *R. canadum* was similarly identified during hyposalinity acclimation, suggesting that *NHE1* can be involved in hyposalinity acclimation in *R. canadum* through the intestine and somatic kidney. Meanwhile, the expression of *NHE1* and *NHE2a* increased in gill with decreasing salinity, but the degree of difference was not significant, and a significant down-regulation was observed in high-salt acclimation. It is speculated that the reduced expression of *NHE1* and *NHE2a* in high salt is to reduce the ion transport efficiency of gill epithelial cells and prevent the decrease of osmotic pressure *in vivo*.

Few studies related to *NKAα3a* have been reported, and it has been suggested that its role in osmolarity regulation is relatively weak compared to *NKAα1a* (Nilsen et al., 2007). In the present study, the expression of *NKAα3a* and *NKAβ1b* in the gills of *R. canadum* decreased significantly with increasing salinity. Similar results could be found in *O. mossambicus* (Feng et al., 2002). As multi-copy genes, *NKAα1a* and *NKAα1b* are often compared together. In the present study, *NKAα1b* was found to be significantly downregulated in both high and low salt suits, in contrast to *NKAα1a* expression pattern. *NKAα1b* was similarly found to be strongly affected by salinity in *O. mossambicus* and *Galaxias rostratus*, similar to *NKAα1a*, further suggesting that *NKAα1* isoforms appear to differ in function (Tipsmark et al., 2011; Urbina et al., 2013). In addition, two *NKAα* isoforms (*NKAα1a* and *NKAα3b*) were highly expressed in the gills after high salt domestication in *L. maculatus*, indicating the importance of *NKAα* isoform genes in the salt stress response of fish (Zhang et al., 2019).

5 Conclusion

In the present study,12 NHE genes and 12 NKA genes were systematically identified from *R. canadum* genome. These genes were found to be distributed across 10 and 9 superscaffolds. NHE and NKA members of *R. canadum* are closest in taxonomic position to teleosts and furthest from mammals, indicating that the protein sequences of both family members are highly conserved in species evolution. The histology of the gills, intestine and kidneys exhibited changes associated with salinity adaptation. Different expression patterns of *R. canadum* NHE genes and NKA genes were displayed in multiple tissues. At the same time, transcriptome sequencing and qPCR results showed that there were differences in the expression patterns of NHE and NKA gene families under different salinities, which provided research data for the osmotic pressure regulation mechanism of *R. canadum*.

Data availability statement

The datasets presented in this study can be found in online repositories. The names of the repository/repositories and accession number(s) can be found below: https://www.ncbi.nlm.nih.gov/, SRP202920 https://www.ncbi.nlm.nih.gov/, PRJNA634421.

Ethics statement

The animal study was reviewed and approved by Institutional Animal Care and Use Committee (IACUC), Fisheries College, Guangdong Ocean University.

Author contributions

ZW, ZC, and BH contributed to conception and design of the study. ZW organized the database. BH performed the statistical analysis. ZC wrote the first draft of the manuscript. ZY, MZ, MJ, and AZ wrote sections of the manuscript. All authors contributed to manuscript revision, read, and approved the submitted version.

Funding

Guangdong University Innovation Team Project (2021KCXTD026, 2022KCXTD013).

Acknowledgments

We are grateful to Guangzhou Genedenovo Biotechnology Co., Ltd for assisting in sequencing and bioinformatics analysis.

Conflict of interest

The authors declare that the research was conducted in the absence of any commercial or financial relationships that could be construed as a potential conflict of interest.

Publisher's note

Supplementary material

The Supplementary Material for this article can be found online at: https://www.frontiersin.org/articles/10.3389/fmars.2023.1228933/full#supplementary-material

References

Ali, A., Azom, M. G., Sarker, B. S., Rani, H., Alam, M. S., and Islam, M. S. (2022). Repercussion of salinity on hematological parameters and tissue morphology of gill and kidney at early life of tilapia. *Aquaculture Fisheries*. doi: 10.1016/j.aaf.2022.04.006

Bailey, T. L., Johnson, J., Grant, C. E., and Noble, W. S. (2015). The MEME suite. *Nucleic Acids Res.* 43, W39–W49. doi: 10.1093/nar/gkv416

Benetti, D. D., Suarez, J., Camperio, J., Hoenig, R. H., Tudela, C. E., Daugherty, Z., et al. (2021). A review on cobia, *Rachycentron canadum*, aquaculture. *J. World Aquaculture Soc.* 52, 691–709. doi: 10.1111/jwas.12810

Berthelot, C., Brunet, F., Chalopin, D., Juanchich, A., Bernard, M., Noël, B., et al. (2014). The rainbow trout genome provides novel insights into evolution after whole-genome duplication in vertebrates. *Nat. Commun.* 5, 3657. doi: 10.1038/ncomms4657

Bystriansky, J. S., Frick, N. T., Richards, J. G., Schulte, P. M., and Ballantyne, J. S. (2007). Failure to up-regulate gill Na+, K+-ATPase α-subunit isoform α1b may limit seawater tolerance of land-locked Arctic char (*Salvelinus alpinus*). *Comp. Biochem. Physiol. Part A: Mol. Integr. Physiol.* 148, 332–338. doi: 10.1016/j.cbpa.2007.05.007

Cao, D. Y., Li, J. F., Huang, B. S., Zhang, J. D., Pan, C. H., Huang, J. S., et al. (2020). RNA-seq analysis reveals divergent adaptive response to hyper- and hypo-salinity in cobia, *Rachycentron canadum*. *Fish Physiol. Biochem.* 46, 1713–1727. doi: 10.1007/s10695-020-00823-7

Chen, G., Wang, Z. L., Wu, Z. H., and Gu, B. H. (2009). Effects of salinity on growth and energy budget of juvenile cobia, r*achycentron canadum*. *J. World Aquaculture Soc.* 40, 374–382. doi: 10.1111/j.1749-7345.2009.00257.x

Chen, S., Zhou, Y., Chen, Y., and Gu, J. (2018). fastp: an ultra-fast all-in-one FASTQ preprocessor. *Bioinformatics* 34, i884–i890. doi: 10.1093/bioinformatics/bty560

Counillon, L., and Pouysségur, J. (2000). The expanding family of eucaryotic Na^+/H^+ exchangers. *J. Biol. Chem.* 275, 1–4. doi: 10.1074/jbc.275.1.1

Dawood, M. A.O., Noreldin, A. E., and Sewilam, H. (2021). Long term salinity disrupts the hepatic function, intestinal health, and gills antioxidative status in Nile tilapia stressed with hypoxia. *Ecotox Environ. Safe* 220, 112412. doi: 10.1016/j.ecoenv.2021.112412

Edwards, S. L., Wall, B. P., Morrison-Shetlar, A., Sligh, S., Weakley, J. C., and Claiborne, J. B. (2005). The effect of environmental hypercapnia and salinity on the expression of NHE-like isoforms in the gills of a euryhaline fish (*Fundulus heteroclitus*). *J. Exp. Zoology Part A: Comp. Exp. Biol.* 303, 464–475. doi: 10.1002/jez.a.175

Feng, S. H., Leu, J. H., Yang, C. H., Fang, M. J., Huang, C. J., and Hwang, P. P. (2002). Gene expression of na^+-k^+-atpase a1 and a3 subunits in gills of the teleost *Oreochromis mossambicus*, adapted to different environmental salinities. *Mar. Biotechnol.* 4, 379–391. doi: 10.1007/s10126-002-0006-0

Figueras, A., Robledo, D., Corvelo, A., Hermida, M., Pereiro, P., Rubiolo, J. A., et al. (2016). Whole genome sequencing of turbot (*Scophthalmus maximus*; Pleuronectiformes): a fish adapted to demersal life. *DNA Res.* 23, 181–192. doi: 10.1093/dnares/dsw007

Fiol, D. F., and Kültz, D. (2007). Osmotic stress sensing and signaling in fishes. *FEBS J.* 274, 5790–5798. doi: 10.1111/j.1742-4658.2007.06099.x

Foskett, J. K., Bern, H. A., Machen, T. E., and Conner, M. (1983). Chloride cells and the hormonal control of teleost fish osmoregulation. *J. Exp. Biol.* 106, 255–281. doi: 10.1242/jeb.106.1.255

Gao, J., Nie, Z. J., Xu, G. C., and Xu, P. (2022). Genome-wide identification of the NHE gene family in Coilia nasus and its response to salinity challenge and ammonia stress. *BMC Genomics* 23, 1–14. doi: 10.1186/s12864-022-08761-9

Gonzalez, R. J. (2012). The physiology of hyper-salinity tolerance in teleost fish: a review. *J. Comp. Physiol. B* 182, 321–329. doi: 10.1007/s00360-011-0624-9

Han, K., Zhou, L., Zeng, X., Zhang, Z., Zou, P., Huang, W., et al. (2022). Effects of low-salinity acclimation on the Na+/K+ ATPase activity and expression of osmoregulatory-related genes in large yellow croaker (*Larimichthys crocea*). *Aquaculture Rep.* 26, 101326. doi: 10.1016/j.aqrep.2022.101326

Holmes, B. J., Williams, S. M., Barnett, A., Awruch, C. A., Currey-Randall, L. M., Ferreira, L. C., et al. (2022). "Research methods for marine and estuarine fishes," in *Wildlife Research in Australia: Practical and Applied Methods* (Australia: Csiro Publishing), 257–286.

Hou, J. L., Chen, L. Q., Zhuang, P., Zhang, L. Z., Tian, H. J., Wang, W., et al. (2006). Structural changes of chloride cells in gills epithelia of juvenile *Acipenser schrenckii* acclimated to various salinities. *J. Fisheries China* 30, 316–322. doi: 10.1360/aps050066

Howe, K., Clark, M. D., Torroja, C. F., Torrance, J., Berthelot, C., Muffato, M., et al. (2013). The zebrafish reference genome sequence and its relationship to the human genome. *Nature* 496, 498–503. doi: 10.1038/nature12111

Hu, Y. C., Chu, K. F., Yang, W. K., and Lee, T. H. (2017). Na^+, K^+-ATPase β1 subunit associates with α1 subunit modulating a "higher-NKA-in-hyposmotic media" response in gills of euryhaline milkfish, Chanos chanos. *J. Comp. Physiol. B* 187, 995–1007. doi: 10.1007/s00360-017-1066-9

Hu, J., Ye, L., Wu, K. C., and Wang, Y. (2016). Effect of acute salinity stress on serum cortisol and activity of Na^+-K^+-ATPase of juvinile *Amphiprion clarkii*. *South. Aquat. Sci. China* 12, 116–120. doi: 10.3969/j.issn.2095-0780.2016.02.017

Huang, S., Li, C. Z., Li, Z. X., Duanzhi, D., Liu, Y. H., Ran, F. X., et al. (2022). Short-term exposure to 5‰ and 15‰ salinity causes the dynamic changes of the NKA gene, enzyme activities and morphological characteristics in fish tissues of *Gymnocypris przewalskii*. *Aquac Res.* 53, 6389–6398. doi: 10.1111/are.16112

Hwang, J., Kim, S., Seo, Y., Lee, K., Park, C., Choi, Y., et al. (2018). Mechanisms of salinity control in sea bass. *Biotechnol. Bioproc E* 23, 271–277. doi: 10.1007/s12257-018-0049-3

Imsland, A. K., Gunnarsson, S., Foss, A., and Stefansson, S. O. (2003). Gill Na^+, K^+-ATPase activity, plasma chloride and osmolality in juvenile turbot (*Scophthalmus maximus*) reared at different temperatures and salinities. *Aquaculture* 218, 671–683. doi: 10.1016/S0044-8486(02)00423-4

Inokuchi, M., Nakamura, M., Miyanishi, H., Hiroi, J., and Kaneko, T. (2017). Functional classification of gill ionocytes and spatiotemporal changes in their distribution after transfer from seawater to fresh water in Japanese seabass. *J. Exp. Biol.* 220, 4720–4732. doi: 10.1242/jeb.167320

Jia, Q., and Lu, W. (2016). Effects of low salinity stress on plasma osmolality, Cortisol, prolactin and growth hormone of Japanese flounder, *Paralichthys olivaceus*. *J. Shanghai Ocean Univ.* 25, 71–77.

Jiang, Y. H., Yuan, C., Qi, M., Liu, Q. G., and Hu, Z. J. (2022). The effect of salinity stress on enzyme activities, histology, and transcriptome of silver carp (*Hypophthalmichthys molitrix*). *Biology* 11, 1580. doi: 10.3390/biology11111580

Kasahara, M., Naruse, K., Sasaki, S., Nakatani, Y., Qu, W., Ahsan, B., et al. (2007). The medaka draft genome and insights into vertebrate genome evolution. *Nature* 447, 714–719. doi: 10.1038/nature05846

Kibenge, F. S., and Strange, R. J. (2021). "Introduction to the anatomy and physiology of the major aquatic animal species in aquaculture," in *Aquaculture Pharmacology* (Netherlands: Elsevier), 1–111.

Kim, D., Langmead, B., and Salzberg, S. L. (2015). HISAT: a fast spliced aligner with low memory requirements. *Nat. Methods* 12, 357–360. doi: 10.1038/nmeth.3317

Kumar, S., Stecher, G., and Tamura, K. (2016). MEGA7: molecular evolutionary genetics analysis version 7.0 for bigger datasets. *Mol. Biol. Evol.* 33, 1870–1874. doi: 10.1093/molbev/msw054

Larsen, P. F., Nielsen, E. E., Meier, K., Olsvik, P. A., Hansen, M. M., and Loeschcke, V. (2012). Differences in salinity tolerance and gene expression between two populations of Atlantic cod (*Gadus morhua*) in response to salinity stress. *Biochem. Genet.* 50, 454–466. doi: 10.1007/s10528-011-9490-0

Li, B., and Dewey, C. N. (2011). RSEM: accurate transcript quantification from RNA-Seq data with or without a reference genome. *BMC Bioinf.* 12, 1–16. doi: 10.1186/1471-2105-12-323

Li, L., Jiang, M., Wang, Y., Wu, Q., Niu, J., and Shen, X. (2014). Effects of low salinity stress on Na+-K+-ATPase activities, expression of Na+-K+-ATPase β-subunit mRNA and microscopical structure in gill filaments of juvenile Mugil cephalus. *J. Zhejiang Univ. (Agriculture Life Sciences)* 40, 223–230. doi: 10.3785/j.issn.1008-9209.2013.09.031

Li, X. J., Shen, Y. D., Bao, Y. G., Wu, Z. X., Yang, B. Q., Jiao, L. F., et al. (2022). Physiological responses and adaptive strategies to acute low-salinity environmental stress of the euryhaline marine fish black seabream (*Acanthopagrus schlegelii*). *Aquat. Toxicol.* 554, 738117. doi: 10.1016/j.aquaculture.2022.738117

Li, H. Y., Zhu, J. Q., Chen, F., and Ding, L. F. (2011). Themorphology of the digestive tract of *Centropristis striata*. *J. Biol. China* 28, 31–34+46. doi: 10.3969/j.issn.2095-1736.2011.04.031

Lin, Y. M., Chen, C. N., and Lee, T. H. (2003). The expression of gill Na, K-ATPase in milkfish, *Chanos chanos*, acclimated to seawater, brackish water and fresh water. *Comp. Biochem. Physiol. Part A: Mol. Integr. Physiol.* 135, 489–497. doi: 10.1016/S1095-6433(03)00136-3

Lin, Y. M., Chen, C. N., Yoshinaga, T., Tsai, S. C., Shen, I. D., and Lee, T. H. (2006). Short-term effects of hyposmotic shock on Na^+/K^+-ATPase expression in gills of the euryhaline milkfish, *Chanos chanos*. *Comp. Biochem. Physiol. Part A: Mol. Integr. Physiol.* 143, 406–415. doi: 10.1016/j.cbpa.2005.12.031

Marshall, W. S. (2011). Mechanosensitive signalling in fish gill and other ion transporting epithelia. *Acta Physiologica* 202, 487–499. doi: 10.1111/j.1748-1716.2010.02189.x

Nilsen, T. O., Ebbesson, L. O., Madsen, S. S., McCormick, S. D., Andersson, E., Björnsson, B. T., et al. (2007). Differential expression of gill Na^+, K^+-ATPaseα-and β-subunits, Na^+, K^+, $2Cl^-$cotransporter and CFTR anion channel in juvenile anadromous and landlocked Atlantic salmon *Salmo salar*. *J. Exp. Biol.* 210, 2885–2896. doi: 10.1242/jeb.002873

Orlowski, J., and Grinstein, S. (2004). Diversity of the mammalian sodium/proton exchanger SLC9 gene family. *Pflügers Archiv* 447, 549–565. doi: 10.1007/s00424-003-1110-3

Pertea, M., Pertea, G. M., Antonescu, C. M., Chang, T.-C., Mendell, J. T., and Salzberg, S. L. (2015). StringTie enables improved reconstruction of a transcriptome from RNA-seq reads. *Nat. Biotechnol.* 33, 290–295. doi: 10.1038/nbt.3122

Robinson, M. D., McCarthy, D. J., and Smyth, G. K. (2010). edgeR: a Bioconductor package for differential expression analysis of digital gene expression data. *bioinformatics* 26, 139–140. doi: 10.1093/bioinformatics/btp616

Sakamoto, T., Uchida, K., and Yokota, S. (2001). Regulation of the ion-transporting mitochondrion-rich cell during adaptation of teleost fishes to different salinities. *Zoological Sci.* 18, 1163–1174. doi: 10.2108/zsj.18.1163

Shaffer, R. V., and Nakamura, E. L. (1989). *Synopsis of biological data on the cobia Rachycentron canadum (Pisces: Rachycentridae)*. USA: NOAA/National Marine Fisheries Service. Available at: http://hdl.handle.net/1834/20527.

Shi, Z. H., Liao, Y. L., Wang, X. S., Zhang, C. J., Peng, S. M., and Gao, Q. X. (2017). Impact of the abrupt salinity decrease on ion-regulation enzyme activity in the gill and serum osmolality from *Epinehelus moara*. *J. Saf. Environ. China* 17, 1210–1214. doi: 10.13637/j.issn.1009-6094.2017.03.074

Smith, H. W. (1932). Water regulation and its evolution in the fishes. *Q. Rev. Biol.* 7, 1–26. doi: 10.1086/394393

Smith, J. W. (1995). Life history of cobia, Rachycentron canadum (Osteichthyes: Rachycentridae), in North Carolina waters. *Brimleyana* 23, 1–23.

Sun, M. L., Jiang, J. L., Wang, L. P., Chen, F., Han, Y. Z., Jiang, Z. Q., et al. (2016). Structural Changes in Gill, Kidney and Intestine of Juvenile *Takifugu rubripes* under Low Salinity Treatment. *J. Guangdong Ocean Univ. China* 36, 38–43. doi: 10.3969/j.issn.1673-9159.2016.06.007

Sundh, H., Nilsen, T. O., Lindström, J., Hasselberg-Frank, L., Stefansson, S. O., McCormick, S. D., et al. (2014). Development of intestinal ion-transporting mechanisms during smoltification and seawater acclimation in Atlantic salmon *Salmo salar*. *J. Fish Biol.* 85, 1227–1252. doi: 10.1111/jfb.12531

Tine, M., Kuhl, H., Gagnaire, P.-A., Louro, B., Desmarais, E., Martins, R. S., et al. (2014). European sea bass genome and its variation provide insights into adaptation to euryhalinity and speciation. *Nat. Commun.* 5, 5770. doi: 10.1038/ncomms6770

Tipsmark, C. K., Breves, J. P., Seale, A. P., Lerner, D. T., Hirano, T., and Grau, E. G. (2011). Switching of Na^+, K^+-ATPase isoforms by salinity and prolactin in the gill of a cichlid fish. *J. Endocrinol.* 209, 237. doi: 10.1530/JOE-10-0495

Upling, J. Y. (2020). A review on the activity of Na^+/K^+-ATPase in branchial ionocytes and its role in salinity adaptation among diadromous species. *World J. Advanced Res. Rev.* 6, 201–211. doi: 10.30574/wjarr.2020.6.2.0158

Urbina, M. A., Schulte, P. M., Bystriansky, J. S., and Glover, C. N. (2013). Differential expression of Na^+, K^+-ATPase α-1 isoforms during seawater acclimation in the amphidromous galaxiid fish *Galaxias maculatus*. *J. Comp. Physiol. B* 183, 345–357. doi: 10.1007/s00360-012-0719-y

Wang, Y., and Hu, X. C. (2009). Microscopical observation on the gill structure of juvenile *Lateolabrax japonicus* under different salinities. *Mar. Sci.* 33, 138–142. doi: 10.1016/j.elecom.2008.10.019

Wang, S. J., Zhang, H. F., Zhao, J., Yang, Y. Q., and Yang, S. S. (2011). Effects of different salinities on growth and physiology of orange-spotted grouper, *epinephelus coioides*. *J. Guangdong Ocean Univ. China* 31, 39–44. doi: 10.3969/j.issn.1673-9159.2011.06.006

Whittamore, J. M. (2012). Osmoregulation and epithelial water transport: lessons from the intestine of marine teleost fish. *J. Comp. Physiol. B* 182, 1–39. doi: 10.1007/s00360-011-0601-3

Yamaguchi, Y., Breves, J. P., Haws, M. C., Lerner, D. T., Grau, E. G., and Seale, A. P. (2018). Acute salinity tolerance and the control of two prolactins and their receptors in the Nile tilapia (*Oreochromis niloticus*) and Mozambique tilapia (*O. mossambicus*): a comparative study. *Gen. Comp. Endocrinol.* 257, 168–176. doi: 10.1016/j.ygcen.2017.06.018

Yan, J. J., Chou, M. Y., Kaneko, T., and Hwang, P. P. (2007). Gene expression of Na^+/H^+ exchanger in zebrafish H^+-ATPase-rich cells during acclimation to low-Na^+ and acidic environments. *Am. J. Physiology-Cell Physiol.* 293, C1814–C1823. doi: 10.1152/ajpcell.00358.2007

Yang, W. K., Chung, C. H., Cheng, H. C., Tang, C. H., and Lee, T. H. (2016). Different expression patterns of renal Na^+/K^+-ATPase α-isoform-like proteins between tilapia and milkfish following salinity challenges. *Comp. Biochem. Physiol. Part B: Biochem. Mol. Biol.* 202, 23–30. doi: 10.1016/j.cbpb.2016.07.008

Yang, J., Xu, W., Geng, L. W., Guan, H. H., Dang, Y. F., and Jiang, H. F. (2014). Effects of salinity on survival,gill and kidney tissue in juveniles of 5 species. *Freshw. Fisheries China* 44, 7–12. doi: 10.13721/j.cnki.dsyy.2014.04.002

Yang, J. R., Yang, J. L., Chen, M. Q., Fu, Z., Sun, J., Yu, G., et al. (2022). Physical responses of Pinctada fucata to salinity stress. *Front. Mar. Sci.* 8. doi: 10.3389/fmars.2021.792179

Yu, N., Li, J., Ou, Y. J., Wang, Y. C., and Su, H. (2012). Structural changes in gill and kidney of juvenile grey mullet under different salinity. *Ecol. Sci. China* 31, 424–428.

Zhang, J. S., Liu, Z. F., Ma, A. J., Cui, W. X., and Qu, J. B. (2020). Response of aquaporin (AQP1, AQP3) and ion channel protein (CFTR, NHE1) of turbot (*Scophthalmus maximus*) to low-salinity stress. *Prog. IN FISHERY Sci. OF China* 41, 41–49. doi: 10.19663/j.issn2095-9869.20190410003

Zhang, X. Y., Wen, H. S., Qi, X., Zhang, K. Q., Liu, Y., Fan, H. Y., et al. (2019). Na+-K+-ATPase and nka genes in spotted sea bass (*Lateolabrax maculatus*) and their involvement in salinity adaptation. *Comp. Biochem. Physiol. Part A: Mol. Integr. Physiol.* 235, 69–81. doi: 10.1016/j.cbpa.2019.05.017

Zhang, X. Y., Wen, H. S., Wang, H. L., Ren, Y. Y., Zhao, J., and Li, Y. (2017). RNA-Seq analysis of salinity stress–responsive transcriptome in the liver of spotted sea bass (*Lateolabrax maculatus*). *PloS One* 12, e0173238. doi: 10.1371/journal.pone.0173238

Zhang, X. Y., Wen, H. S., Zhang, K. Q., Liu, Y., Fang, X., and Li, Y. (2018). Analysis of the isotonic point and effects of seawater desalination on the Na^+/K^+ /Cl concentration, Na^+-K^+ -ATPase activity and relative gene expressions in *Lateolabrax maculatus*. *J. Fisheries China* 42, 1199–1208. doi: 10.11964/jfc.20170410780

Zhou, Q. C., Wu, Z. H., Tan, B. P., Chi, S. Y., and Yang, Q. H. (2006). Optimal dietary methionine requirement for juvenile cobia (*Rachycentron canadum*). *Aquaculture* 258, 551–557. doi: 10.1016/j.aquaculture.2006.03.035